Apoptosis (2019) 24:278–289
https://doi.org/10.1007/s10495-019-01517-z

Overexpression of augmenter of liver regeneration (ALR) mitigates the effect of H_2O_2-induced endoplasmic reticulum stress in renal tubule epithelial cells

Xiao Jiang[1] · Xiao-hui Liao[1] · Li-li Huang[1] · Hang Sun[2] · Qi Liu[2] · Ling Zhang[1]

Published online: 24 January 2019

Abstract

Ischemia/reperfusion is a major cause of acute kidney injury and can induce apoptosis in renal epithelial tubule (HK-2) cells. Accumulating evidence indicates that endoplasmic reticulum (ER) stress is a major contributor to apoptosis in acute kidney injury. We previously reported that augmenter of liver regeneration (ALR) functions as an anti-apoptotic factor in H_2O_2-treated HK-2 cells although the precise mechanism underlying this action remains unclear. In the present study, we investigate the role of ALR in H_2O_2-induced ER stress-mediated apoptosis. We overexpressed ALR and established a H_2O_2-induced ER stress model in HK-2 cells. Overexpression of ALR reduced the level of reactive oxygen species and the rate of apoptosis in H_2O_2-treated HK-2 cells. Using confocal microscopy and western blot, we observed that ALR colocalized with the ER and mitochondria compartment. Moreover, ALR suppressed ER stress by maintaining the morphology of the ER and reducing the levels of the ER-related proteins, glucose-regulated protein 78 (GRP78), phospho-protein kinase-like ER kinase (p-PERK), phospho-eukaryotic initiation factor 2α (p-eIF2α) and C/EBP-homologous protein (CHOP) significantly ($p < 0.05$). Mechanistically, ALR promoted Bcl-2 expression and suppressed Bax and cleaved-caspase-3 expression significantly during ER-stress induced apoptosis ($p < 0.05$). Furthermore, ALR attenuated calcium release from the ER, and transfer to mitochondria, under ER stress. To conclude, ALR alleviates H_2O_2-induced ER stress-mediated apoptosis in HK-2 cells by suppressing ER stress response and by maintaining calcium homeostasis. Consequently, ALR may protect renal tubule epithelial cells from ischemia/reperfusion induced acute kidney injury.

Keywords Augmenter of liver regeneration · Endoplasmic reticulum stress · Apoptosis · Acute kidney injury

Introduction

Acute kidney injury (AKI), also known as acute renal failure, is a severe clinical syndrome characterized by a rapid loss of renal function [1]. With high morbidity and mortality, AKI is a challenge for clinicians both in the hospital and the community. A range of factors can lead to AKI, including ischemic reperfusion (I/R) insult, sepsis and systemic inflammation [2]. Renal I/R is a major cause of AKI characterized by cell death in the kidney by apoptosis and necroptosis, particularly in the proximal renal tubule epithelial cells [3]. It is well accepted that reactive oxygen species (ROS) play an important role in renal I/R injury [4] which is known to promote the formation of ROS, such as the free radicals superoxide anion ($O_2^{\cdot -}$) and hydroxyl radical ($OH^{\cdot}$), and the non-radical oxidants, hydrogen peroxide (H_2O_2), hypochlorous acid (HOCl) and peroxynitrite (ONOO−) [5]. The excessive production of ROS in ischemia/reperfusion-induced AKI causes oxidative damage in renal tubule cells, including endoplasmic reticulum (ER) stress and mitochondrial dysfunction; these changes ultimately lead to apoptosis or necrosis [6].

Although the molecular mechanism underlying renal tubule cell apoptosis in renal ischemia/reperfusion injury is still poorly understood, there is increasing evidence suggests

✉ Ling Zhang
zhangling@hospital.cqmu.edu.cn

1 Department of Nephrology, Second Affiliated Hospital of Chongqing Medical University, Chongqing 400010, China

2 Key Laboratory of Molecular Biology for Infectious Diseases (Ministry of Education), Institute for Viral Hepatitis, Department of Infectious Diseases, Second Affiliated Hospital of Chongqing Medical University, Chongqing 400010, China

that ER stress may play a role in apoptosis caused by renal I/R injury [7–9]. The ER is a multifunctional organelle responsible for protein folding, modification and cellular calcium homeostasis. Specific proteins are folded, maturated and assembled in the endoplasmic reticulum [10]. However, cellular stresses such as ischemia, oxidative stress, hypoxia and glucose deprivation can cause ER stress. In addition, when ER stress occurs, unfolded or misfolded proteins can accumulate in ER, which triggers a series of responses referred to as the unfolded protein response (UPR) [6]. There are three major transmembrane sensors that mediate the UPR pathway in order to maintain ER homeostasis. These sensors are activated protein kinase-like ER kinase (PERK), inositolrequiring enzyme 1α (IRE1α) and activating transcription factor 6 (ATF6). In normal conditions, the sensors are bound to the ER molecular chaperone, glucose-regulated protein 78 (GRP78). Once unfolded proteins accumulate, GRP78 dissociates from these sensors and triggers the UPR. At the beginning, the UPR helps to maintain the function of the ER. However, prolonged ER stress leads to cell apoptosis or necrosis. C/EBP homologous protein (CHOP) is a major pro-apoptotic protein that is induced by prolonged ER stress, and contributes to apoptosis by regulating the Bcl-2 family and subsequently activates the caspase dependent pathway of apoptosis [11]. Moreover, the ER is the major organelle responsible for calcium storage. Studies have shown that disordered calcium homeostasis under ER stress plays an important role in apoptosis induced by ER stress [12, 13]. Under ER stress, calcium is released from the ER and accumulates in mitochondria causing mitochondrial Ca^{2+} overload, which then causes the outer membrane of the mitochondria to become permeabilized and subsequently triggers apoptosis in the mitochondrial pathway [14].

Augmenter of liver regeneration (ALR, also known as GFER) is a fundamental life protein which plays a key role in physiological and pathophysiology activity such as energy transduction, cell survival and regeneration, metabolic homeostasis, iron metabolism and stem cell maintenance [15]. ALR was first found in hepatocyte cytosol and had the capacity to augment regeneration of the liver after hepatectomy [16]. Accumulating evidence showed that ALR is expressed ubiquitously in all organs, including the kidney [17, 18]. ALR is expressed as a short form (15 kDa) and a long form (23 kDa). The short form of ALR is mainly secreted from hepatocytes into the extracellular environment while the long form of ALR is reported to localize intracellularly. ALR is present in different subcellular structures, including mitochondria, cytosol, endoplasmic reticulum, and nucleus [19]. Previous study investigated the role of ALR on mitochondria since ALR is homologous with the yeast ERV1 gene which encoding an essential mitochondrial matrix protein in yeast [20]. Moreover, ALR also shares significant homology to yeast gene ERV2 which is reported as a flavoprotein oxidase located in the ER [21]. However, little is known on the role of ALR on the ER. Increasing evidence has shown that ALR has an anti-apoptotic effect [22]. Our previous study showed that ALR promotes renal function in rats subjected to ischemia/reperfusion in vivo [17]. Furthermore, we investigated how ALR protects human renal tubule cells from apoptosis induced by H_2O_2 in vitro [23]. Nevertheless, the mechanisms underlying the effect of ALR against apoptosis remains poorly understood.

While ER stress plays an important role in apoptosis, little is known about the role of ALR in H_2O_2-induced ER stress-mediated apoptosis. In the present study, we established a H_2O_2-induced ER stress cell model and overexpressed ALR in HK-2 cells in order to investigate the role of ALR in H_2O_2-induced ER stress and whether ALR modulates apoptosis via the ER-stress pathway.

Materials and methods

Cell culture, treatment and cell survival

The human renal tubule epithelial (HK-2) cell line was purchased from ATCC and cultivated in Roswell Park Memorial Institute (RPMI) 1640 medium (Gibco, USA) supplemented with 10% fetal bovine serum (BI, Israel), 100 IU/mL penicillin and 100 mg/mL streptomycin (Invitrogen, USA) at 37 °C in a 5% CO_2 atmosphere. We established a H_2O_2-induced ER stress cell model as previously described [24]. H_2O_2 (Chuandong, China) was added to the medium to induce cellular ER stress. Different concentrations of H_2O_2 (100 μM, 200 μM or 400 μM) were incubated for different time periods (6 h, 12 h and 24 h) in order to decide upon the optimal conditions. The Cell Counting Kit-8 (CCK-8) kit (Dojindo, Japan) was used to determine the cell survival rate. The experiment was performed according to manufacturer's instructions.

Lentiviral infection

The full length of the *ALR* gene (*GFER*, NM_005262) was synthesized using a human cDNA library. The sequences (shown below) were then cloned into a lentiviral vector GV287 (GeneChem, Shanghai, China). At 40% confluence, HK-2 cells were infected with the Lenti-ALR-EGFP (hereafter referred to as ALR overexpression, ALR-OE) or Lenti-EGFP (hereafter referred to as vector). After 72 h, transduction efficiency was assessed by fluorescent microscopy. The expression of ALR was confirmed by real-time polymerase chain reaction (PCR) and western blot analysis. The sequences used to clone the full length *ALR* gene were as follows:

Forward primer 5′-ATCGGGATCCCGCCACCATGG CGGCGCCCGGCGA-3′ and

Reverse primer 5′-CGGGTACCGGTGTCACAGGAG CCATCCTTC-3′

Isolation of ER and mitochondria

Isolation of the ER was performed with an ER protein extraction kit (BestBio, Shanghai, China) in accordance with the manufacturer's guidelines. In brief, cells were harvested after centrifugation at 500×*g* for 5 min and then washed with ice-cold phosphate buffer saline (PBS). A Dounce homogenizer was then used to fully homogenize cells after adding Solution A from the kit. After centrifugation at 1000×*g* for 10 min at 4 °C, the supernatant was collected, transferred to an ice-cold tube, and centrifuged at 12,000×*g* for 10 min at 4 °C. Subsequently, the supernatant was transferred to a fresh tube and centrifuged at 45,000×*g* for 45 min at 4 °C. The pellet, was then resuspended in Solution B from the kit and then centrifuged at 45,000×*g* for another 45 min at 4 °C. Finally, the pellet was resuspended in Solution C and contained the ER proteins; mitochondrial fractions were performed with a mitochondrial protein extraction kit (BestBio, Shanghai, China) and isolated according to manufacturer's instructions.

Confocal microscopy

To investigate the subcellular distribution of ALR in renal tubule cells, HK-2 cells were plated onto a glass-bottomed dish (NEST, China) for confocal microscopy observation. After attachment, the cells were fixed with 4% paraformaldehyde, permeabilized with 0.1% Triton X-100, blocked with 10% albumin from bovine serum (BSA) and incubated with primary antibody (anti-ALR, 1:200; Santa Cruz, USA) overnight at 4 °C and then incubated with Cy5-conjugated goat anti-mouse IgG antibody (1:100, Ex/Em = 649 nm/670 nm; Bioss China) at room temperature for 60 min. Next, an ER-Tracker (Beyotime, China) Red fluorescent probe (Ex/Em = 587 nm/615 nm) was added in accordance with the manufacturer's instructions. For mitochondria staining, the MitoTracker Red CMXRos (Ex/Em = 579 nm/599 nm; Yeasen, China) was added before fixation with 4% paraformaldehyde. Finally, 4′,6-diamidino-2-phenylindole (DAPI) (1 μg/mL) was added to stain the nucleus and the dishes were mounted with 60% glycerol for subsequent observation. The dishes were washed with PBS between each step. Confocal fluorescence images were acquired using a Nikon A1R confocal unit mounted on a Ti2000 inverted microscope controlled by NIS elements acquisition software (Nikon, USA) and using an oil immersion objective.

Real-time polymerase chain reaction (PCR)

Total RNA was extracted from HK-2 cells using the Total RNA Extraction kits (BioTeke, Beijing, China). Total RNA was reverse-transcribed to cDNA using the PrimeScript™ II Reverse Transcriptase kit (TaKaRa, Japan). Real-time PCR was performed using the SYBR Premix (TaKaRa, Japan). For quantitative analysis, the ALR gene, along with GAPDH as a positive control, was amplified by the SYBR Premix using the CFX Connect Real-Time system (Bio-Rad, CA, USA). Relative gene expression was then analyzed using CFX Manager. Primer sequences were as follows:

ALR-F 5′-GTGAGGAGTGTGCTGAAGACC-3′; ALR-R 5′-TGAGCAGTCGAAGTCAGGCTTG-3′;

GAPDH-F 5′-TGACTTCAACAGCGACACCCA-3′ and GAPDH-R 5′-CACCCTGTTGCTGTAGCCAAA-3′.

Western blotting

Proteins were extracted by RIPA lysis buffer (Beyotime, China) and quantified using a Bicinchoninic Acid (BCA) kit (Beyotime, China). Briefly, western blot analyses were then performed according to standard protocol described previously [23]. The following primary antibodies were used: anti-ALR (1:1000) (Santa Cruz, USA), anti-Phospho-PERK (1:1000) (Biolegend, USA), anti-β-actin (Proteintech, USA), anti-Calnexin (1:1000), anti-COX IV (1:1000), anti-GRP78 (1:1000), anti-PERK (1:1000), anti-eIF2α (1:1000), anti-Phospho-eIF2α (1:1000), anti-CHOP (1:1000), anti-Bax (1:1000), anti-Bcl-2 (1:1000), anti-cleaved-caspase-3 (1:1000) from Cell Signaling Technology. Then, corresponding horseradish peroxide (HRP)-conjugated secondary antibodies (1:10,000) (Cell Signaling Technology, USA) were applied and an enhanced chemiluminescence (ECL) kit (Keygen, China) was used to detect immunoreactive bands with a ChemiDoc Imaging System (Bio-Rad,CA, USA).

Transmission electron microscopy

After incubation with 200 μM of H_2O_2 for 12 h, the cells were harvested gently and fixed with 2.5% glutaraldehyde in 0.1 M PBS (pH 7.4). The cells were then post-fixed with 1% osmium tetraoxide in PBS and dehydrated with a series of ethanol solutions and embedded in epoxy resin. Ultrathin samples were then prepared by sectioning and examined at 80 kV using an H-7100 transmission electron microscope (Hitachi, Japan).

Detection of ROS and apoptosis by flow cytometry

Intracellular ROS levels were detected by dihydroethidium (DHE) (Ex/Em = 518 nm/605 nm; Keygen, China). After treatment with H_2O_2, cells were harvested and exposed to

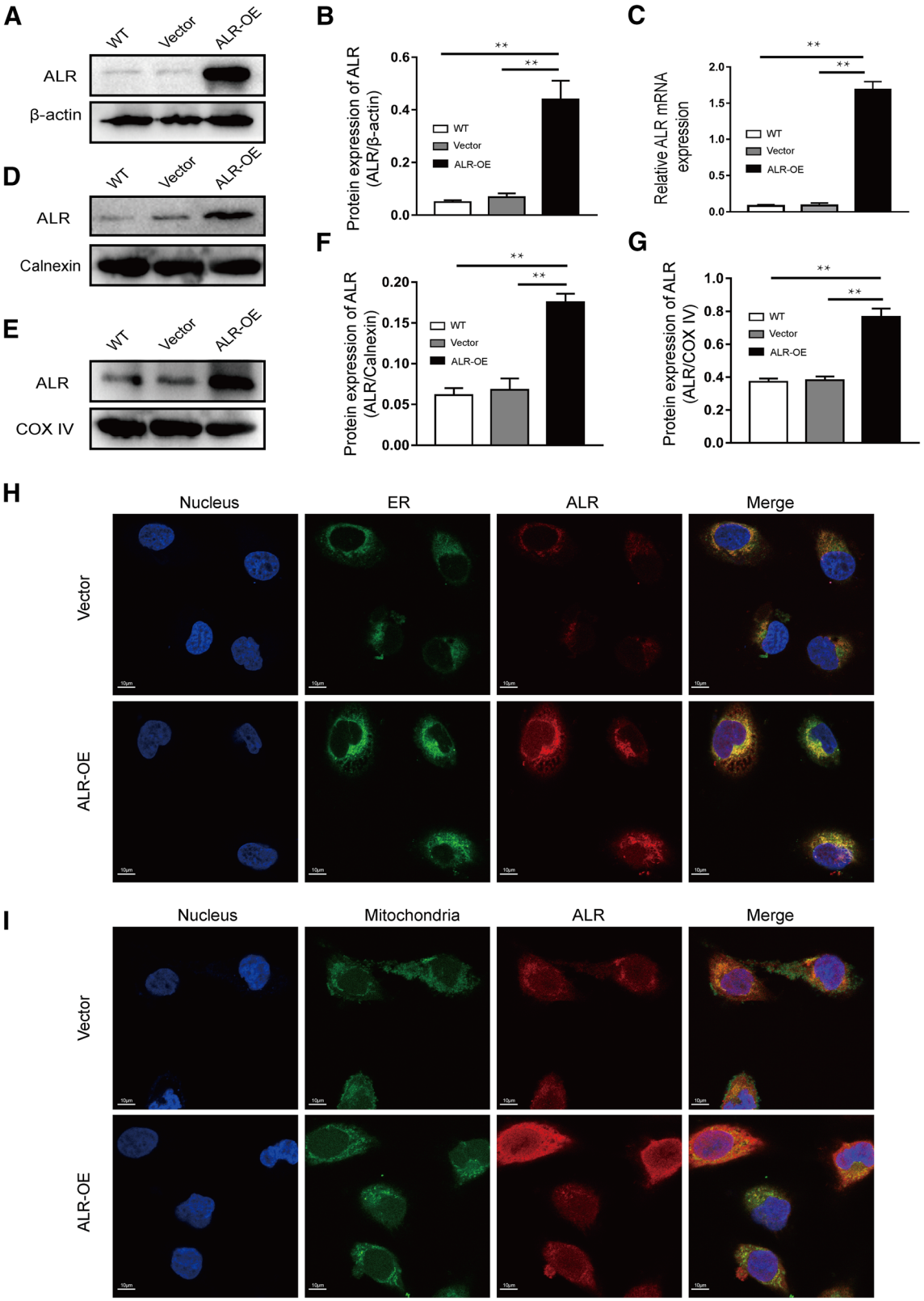

DHE (50 μM final concentration) for 30 min at 37 °C in the dark. Then, cells were washed gently with RPMI 1640 three times. 6×10^4 events (cells) were recorded by the flow cytometer for each sample. The apoptosis rate of HK-2 cells treated with H_2O_2 was then determined using the PE Annexin V staining Kit (BD, USA). Cells were washed twice

◂**Fig. 1** Expression and distribution of ALR in the ER and mitochondria. **a** Western blots of ALR protein expression of HK-2 cells in the WT, vector and ALR-OE group. **b** The bar graph shows intensity of ALR protein expression of ALR-OE group compared with that of vector or WT group. **c** The bar graph shows relative mRNA expression of ALR in the WT, vector and ALR-OE HK-2 cells. **d** Western blots of ALR protein expression in the ER fraction of HK-2 cells in the WT, vector and ALR-OE group. **f** The bar graph shows intensity of ALR protein expression in the ER fraction of ALR-OE group compared with that of vector or WT group. **e** Western blots of ALR protein expression in the mitochondria fraction of HK-2 cells in the WT, vector and ALR-OE group. **g** The bar graph shows intensity of ALR protein expression in the mitochondria fraction of ALR-OE group compared with that of vector or WT group. **h, i** Immunofluorescence experiment was performed to detect ALR, ER and mitochondria in the HK-2 cells. Blue, DAPI; green, ER-Tracker or MitoTracker Red CMXRos; red, ALR; yellow, co-localization section. ** means $p < 0.05$. (Color figure online)

with cold PBS and then resuspended in 1 × Binding Buffer at a concentration of 1×10^6 cells/mL. Cells were incubated with 5 μL of PE Annexin V and 5 μL 7-AAD for 15 min at room temperature in the dark. In total, 1×10^4 events (cells) were recorded by the flow cytometer for each sample. Fluorescence data were measured and analyzed on FACS Canto II software (BD, USA).

Detection of calcium

Cells were plated onto a six-well plate for fluorescence microscopy observation or a 96-well plate for microplate reader testing. After attachment, the cells were mixed with 200 μM of H_2O_2 for 12 h. Then Hank's Balanced Salt Solution (devoid of Ca^{2+} and Mg^{2+}), without phenol red and containing a final concentration of 5 μM Rhod 2-AM (Dojindo, Japan), was added directly to the cells for 30 min at 37 °C. The Rhod 2-AM working solution (dissolved in dimethyl sulfoxide) was mixed with 0.05% Pluronic F127 (Beyotime) and 2.5 mM of probenecid for better permeability. The fluorescence signal (Ex/Em = 557 nm/581 nm) was measured by fluorescence microscopy (Nikon) or the Varioskan LUX multimode microplate reader (Thermo Fisher Scientifc, USA). For microscopy detection, images were acquired every 2 s for 10 min continuously using Nikon NIS-Elements software. The fluorescence intensity was analyzed by ImageJ software. For each kinetic measurement, the readings (300 readings in 10 min) were acquired and analyzed by Thermo Scientifc SkanIt™ software. The experiment was performed in triplicate and averaged in the graph.

Statistical analysis

Each experiment was performed three times separately. Data are presented as means ± standard deviation (SD). Statistical analyses were performed using the Student's *t* test for individual comparisons. Differences were considered to be statistically significant when $p < 0.05$.

Results

Expression of ALR in the cytoplasm, mitochondria or ER fraction from HK-2 cells

To investigate the role of ALR in HK-2 cells, we overexpressed ALR in HK-2 cells. The HK-2 cells were transfected with a lentiviral vector carrying the human *ALR* gene. The overexpression of ALR was determined by real-time PCR and western blot analysis. PCR results showed that the ALR mRNA levels of the ALR-OE group were significantly increased compared with that of the vector group or wild-type group (WT) (Fig. 1c) ($p < 0.05$). Western blot results showed that the expression level of the ALR protein in the ALR-OE group was significantly higher than that of the vector group or WT group (Fig. 1a, b) ($p < 0.05$). To further explore the subcellular content of ALR, we extracted the ER fraction and the mitochondrial fraction from HK-2 cells. Western blot results showed that the expression level of ALR protein extracted from ER in the ALR-OE group was significantly higher than that of the vector group or WT group (Fig. 1d, f) ($p < 0.05$). Similarly, the expression level of ALR protein extracted from mitochondria in the ALR-OE group was significantly higher than that of the vector group or WT group (Fig. 1e, g) ($p < 0.05$).

Colocalization of ALR with ER or mitochondria in HK-2 cells

To investigate whether ALR colocalizes with the ER or mitochondria in HK-2 cells, we used ER Tracker or MitoTracker to explore the subcellular distribution of ALR. Confocal microscopy results showed that ALR extensively overlapped with the ER compartment in HK-2 cells, particularly in the ALR-OE group (Fig. 1h), which indicated that ALR colocalized with the ER in HK-2 cells. Meanwhile, confocal analysis of mitochondria and ALR showed that ALR was colocalized in mitochondria (Fig. 1i).

Cell survival and the expression of ALR in HK-2 cells after H_2O_2 treatment

To construct a cell model of oxidative stress-induced ER stress, we treated HK-2 cells with different concentrations of H_2O_2 (100 μM, 200 μM and 400 μM) at different durations (6 h, 12 h and 24 h). We then tested cell survival rate using a Cell Counting Kit-8 to determine the optimal conditions for H_2O_2 treatment. In all three groups, the cell survival rates were decreased in a dose- and

time-dependent manner. When treated with 100 μM or 400 μM of H_2O_2, the cell survival rates among the three groups were not significantly different (Fig. 2a). However, when treated with 200 μM of H_2O_2, the ALR-OE group showed a significantly higher cell survival rate from 6 to 24 h, compared with that of the vector group or WT group ($p < 0.05$). Therefore, we chose 200 μM of H_2O_2 as the optimal condition for subsequent experiments.

To further investigate whether ALR was involved in H_2O_2-induced ER stress, the expression of ALR protein was determined in WT HK-2 cells after treatment with 200 μM of H_2O_2. We found that ALR protein expression gradually increased at 12 h, compared with cells without H_2O_2 treatment ($p < 0.05$), and decreased after 48 h compared with the expression at 12 h (Fig. 2b, c) ($p < 0.05$). These changes in ALR protein expression indicated that ALR might be involved in the process of ER stress.

Detection of ROS in HK-2 cells after H_2O_2 treatment

ROS is the major factor underlying oxidative stress. To further evaluate the effect of ALR on H_2O_2-induced oxidative stress, we measured the levels of intracellular ROS by DHE, an indicator of peroxide. Results showed that the DHE fluorescence intensity of cells exposed to H_2O_2 was stronger than that without H_2O_2 exposure (Fig. 3a, b) ($p < 0.05$), which indicated that ROS was predominantly generated in the presence of H_2O_2. With prolonged exposure time, the fluorescence intensity was increased in a time-dependent manner (Fig. 3a) ($p < 0.05$), which showed that ROS accumulated over time. Furthermore, at the three-time points

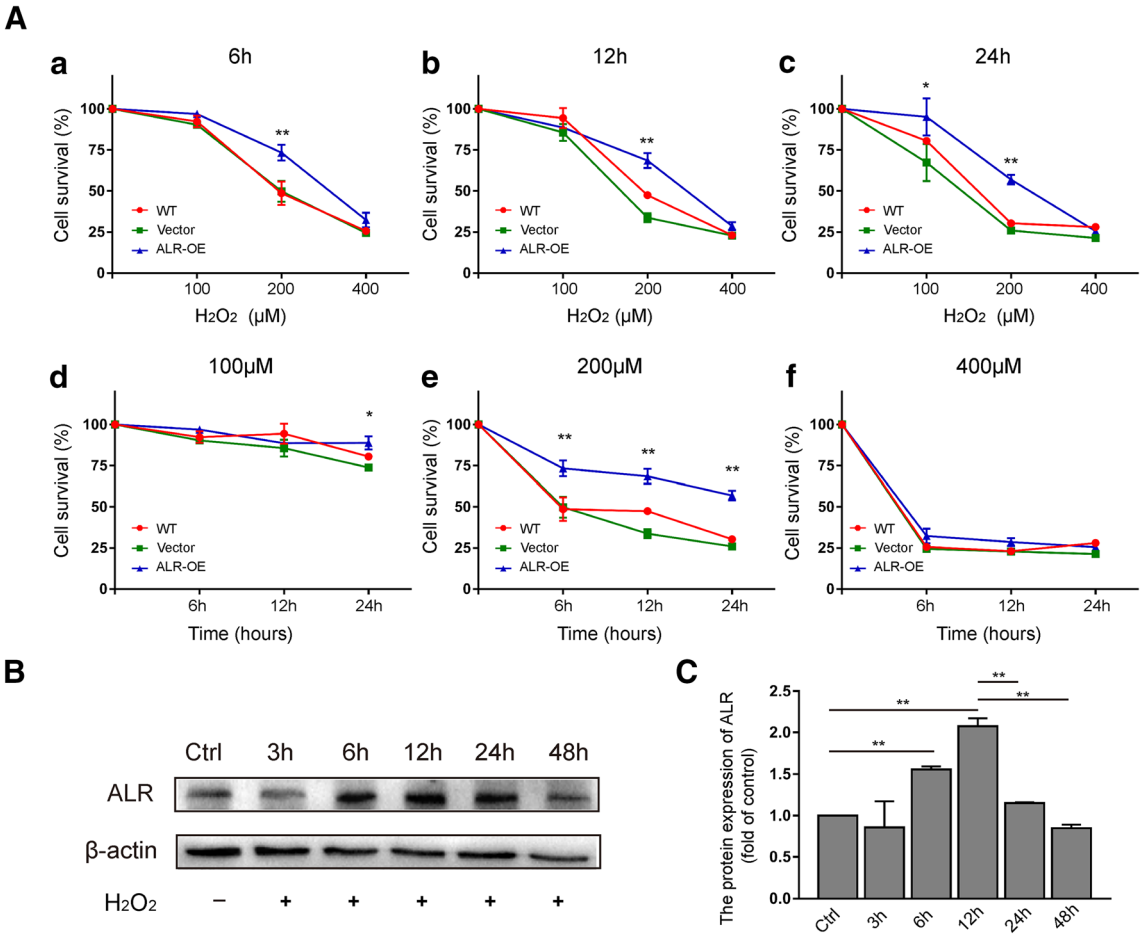

Fig. 2 Cell survival and expression of ALR under H_2O_2 insult. **a** Cell survival rates of HK-2 cells after exposure to different dosages of H_2O_2 (100 μM, 200 μM and 400 μM) for different time (6 h, 12 h and 24 h) using the Cell Counting Kit-8 assay. Red circle represent WT group; green square, vector group; blue triangle, ALR-OE group. The concentration curve (a, b, c) and time curve (e, f, g) showed that cell survival rates of ALR-OE group was higher than that of WT or vector group. **b** Western blots of ALR protein expression in the wild type HK-2 cells after treatment of 200 μM H_2O_2 for different time (3 h, 6 h, 12 h, 24 h and 48 h). **c** The bar graph shows intensity of ALR protein in the wild type HK-2 cells after treatment of 200 μM H_2O_2 for different time (3 h, 6 h, 12 h, 24 h and 48 h). The horizontal lines show which groups are compared. * means $p < 0.05$. ** means $p < 0.01$. (Color figure online)

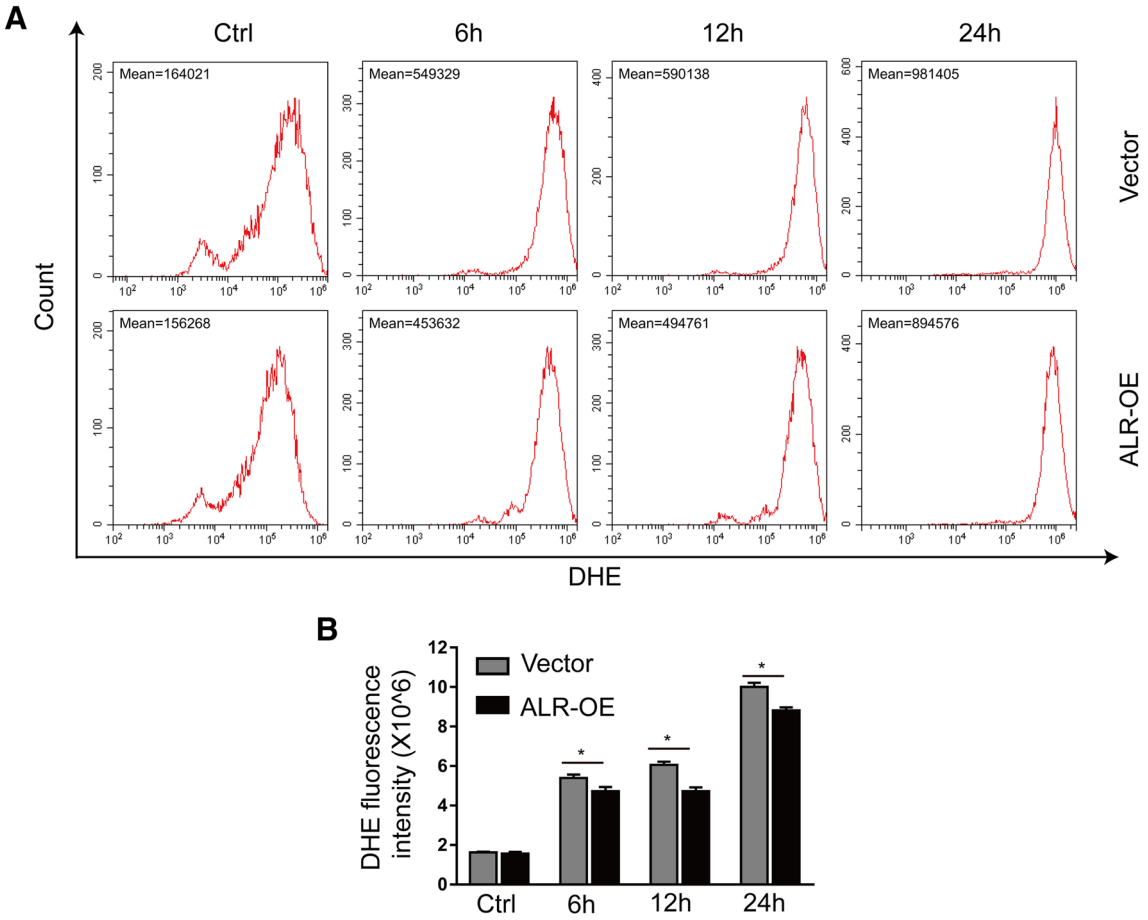

Fig. 3 The level of ROS in HK-2 cells under H_2O_2 insult. **a** Quantification of the ROS level in HK-2 cells by DHE staining using flow cytometer (FCM). The mean fluorescence intensity of DHE was showed on the left top of each FCM image. The cells were treated with 200 μM H_2O_2 for different time (6 h, 12 h, and 24 h) in vector and ALR-OE group, respectively. The cells without H_2O_2 treatment was as control (Ctrl). **b** The bar graph shows the statistical analysis of DHE fluorescence intensity. * means $p < 0.05$

(6 h, 12 h and 24 h), the fluorescence intensity of the ALR-OE group was significantly decreased compared with that of the vector group (Fig. 3b) ($p < 0.05$).

Apoptosis rate of HK-2 cells after H_2O_2 treatment

Since ER stress can eventually cause cell apoptosis, we determined the apoptosis rate in HK-2 cells induced by ER stress using PE Annexin V and 7-AAD staining. When exposed to H_2O_2 for 6 h, 12 h and 24 h, the proportion (%) of apoptotic cells in the vector group (61.21% ± 3.20%, 67.87% ± 1.48% and 88.73% ± 2.20%) was higher than that of the ALR-OE group (23.50% ± 2.30%, 27.13% ± 2.17% and 76.46% ± 1.42%) (Fig. 4a, b) ($p < 0.05$).

Effect of ALR on H_2O_2-induced ER stress

To explore ER stress induced by H_2O_2 treatment and whether the overexpression of ALR can protect HK-2 cells from ER stress, we investigated the morphology of the ER by TEM. We found that the structure of the ER was well distinguished in PBS-treated cells, while the lumen of ER in the H_2O_2 treated cells were dilated, both in the ALR-OE group and the vector group. However, the lumen of ER in the ALR-OE group were dilated to a lesser extent than that of the vector group (Fig. 4c).

Having found that ALR alleviated the ER structural problems induced by H_2O_2, we further investigated whether ALR attenuated the H_2O_2-triggered ER stress pathway. Cells were incubated with H_2O_2 and the expression of ER chaperones and UPR target genes were detected by western blot assay. After treatment with H_2O_2, we found that the protein expression of GRP78 was significantly decreased in the ALR-OE group compared with that of the vector group (Fig. 5a, b) ($p < 0.05$). Furthermore, the phosphorylation of PERK or eIF2α was significantly upregulated in the vector group ($p < 0.05$), compared with that of the ALR-OE group (Fig. 5a, c, d). In addition, the expression of CHOP, a critical

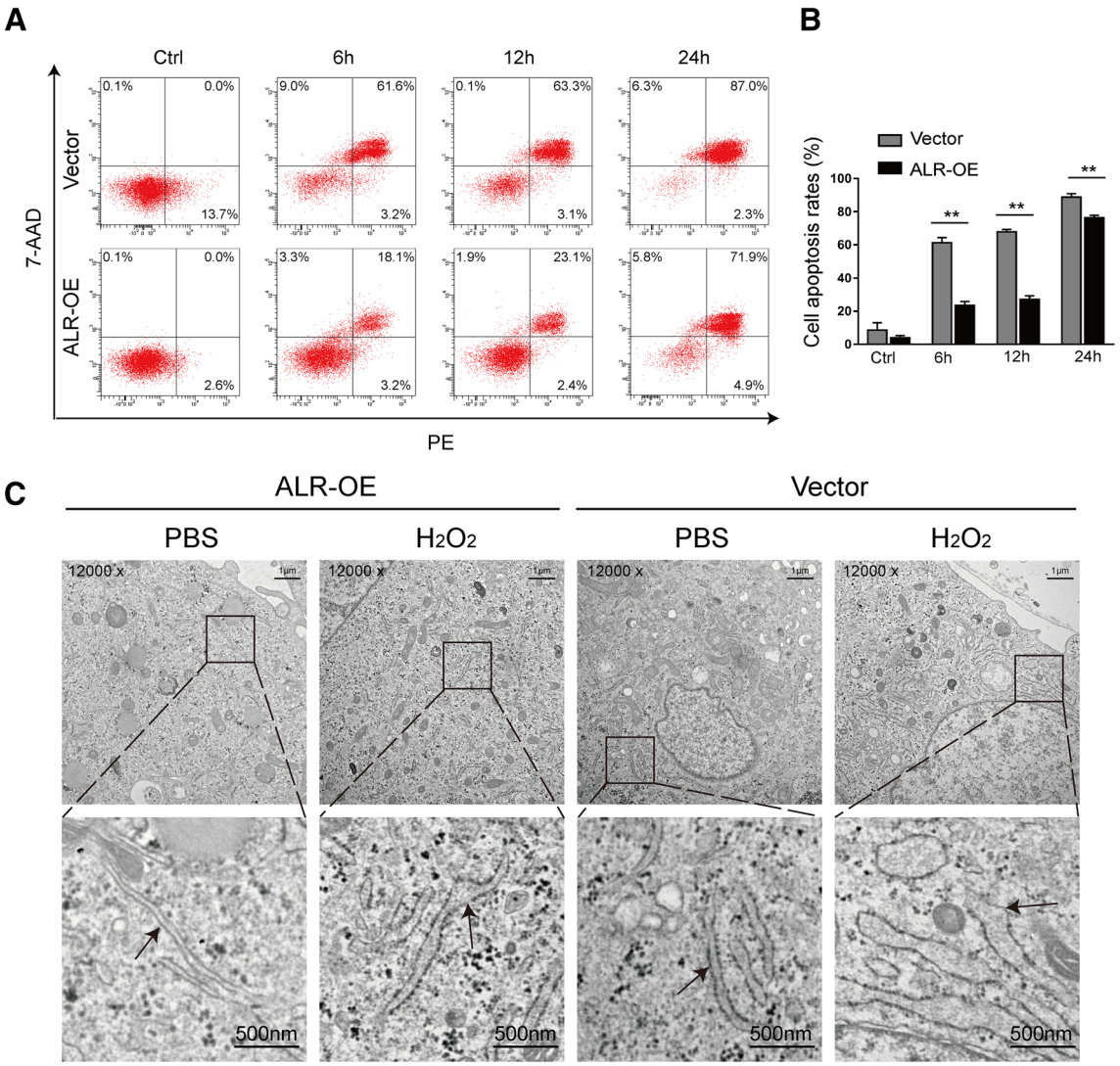

Fig. 4 ALR attenuates apoptosis and maintains the morphology of ER in HK-2 cells under H_2O_2 insult. **a** The vector and ALR-OE cells were treated with 200 μM H_2O_2 for 6 h, 12 h and 24 h respectively and the cells without H_2O_2 exposure were as control (Ctrl). The apoptotic cells were detected by PE Annexin V and 7-AAD. Cells that are considered viable are PE Annexin V negative and 7-AAD negative; cells in early apoptosis are PE Annexin V positive and 7-AAD negative; and cells in late apoptosis or already dead are both PE Annexin V and 7-AAD positive. **b** The bar graph shows apoptosis rates, the proportion (%) of apoptotic cells (right upper quadrant and right upper quadrant), in vector group and ALR-OE group. **c** The transmission electron microscope observation of ER morphology of HK-2 cells with PBS or H_2O_2 treatment in vector group or ALR-OE group. The images in the lower row showed the amplification of the ER morphology of the upper row. The arrows indicate the ER lumen. ** means $p < 0.01$

mediator of ER stress-induced apoptosis, was significantly up-regulated in the vector group, compared with that of the ALR-OE group (Fig. 5a, e) ($p < 0.05$). Collectively, these results suggest that the overexpression of ALR can alleviate ER stress under H_2O_2 insult.

Effect of ALR upon the apoptosis pathway

Since CHOP regulates the intrinsic apoptosis pathway via the inhibition of Bcl-2, we determined the expression levels of the proapoptotic protein Bax and anti-apoptotic proteins Bcl-2. Treatment with H_2O_2 increased Bax expression in both groups, but particularly in the vector group compared with that of the ALR-OE group (Fig. 6a). The expression of bcl-2 decreased in both groups under H_2O_2 insult ($p < 0.05$), and the expression of bcl-2 protein decreased to a lesser extent in the ALR-OE group compared with that of the vector group (Fig. 6a) ($p < 0.05$). As a consequence, the ratio of Bax to Bcl-2 protein was upregulated significantly in the vector group compared with the ALR-OE group (Fig. 6b) ($p < 0.05$). Furthermore,

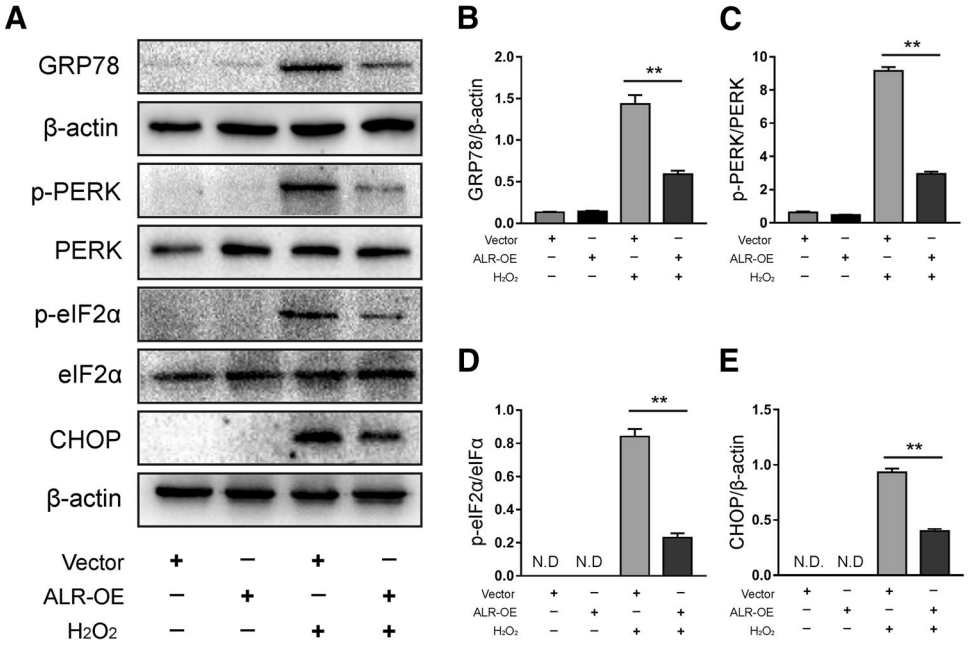

Fig. 5 Effect of ALR on H_2O_2-induced ER stress. **a** Western blots of ER stress-related proteins, GRP78, p-PERK, PERK, p-eIF2α, eIF2α and CHOP, in ALR-OE group or vector group with or without H_2O_2. **b** The bar graph exhibits relative protein expression of GRP78 normalized by β-actin. **c** The bar graph exhibits phospho-PERK/PERK ratio. **d** Graph exhibits phospho-eIF2α/eIF2α ratio. N.D. means not detected. **e** The bar graph exhibits relative protein expression of CHOP normalized by β-actin. N.D. means not detected. ** means $p < 0.01$

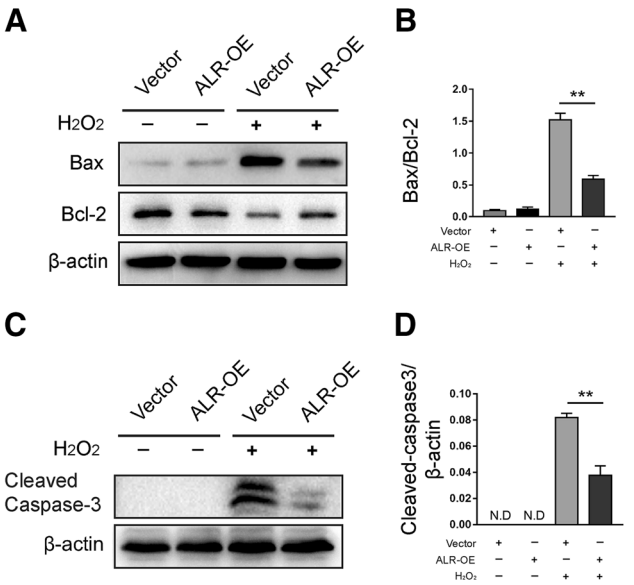

Fig. 6 Effect of ALR on H_2O_2-induced apoptosis-related proteins. **a** Western blots of Bax and Bcl-2 in ALR-OE group or vector group with or without H_2O_2. **b** The bar graph exhibits Bax/Bcl-2 ratio. **c** Western blots of cleaved caspase-3. **d** The bar graph exhibits cleaved caspase-3/β-actin ratio. N.D. means not detected. ** means $p < 0.01$

we identified evidence for the activation of caspase-3, a crucial mediator of apoptosis. After treatment with H_2O_2 for 12 h, the expression of cleaved caspase-3 was upregulated significantly in the vector group compared to the ALR-OE group (Fig. 6c, d) ($p < 0.05$). Cleaved caspase-3 was not detected in HK-2 cells without H_2O_2 treatment (Fig. 6c, d).

Effect of ALR on calcium release

To investigate the possible role of ALR in the Ca^{2+} equilibrium of ER, we performed a preliminary experiment to detect the changes in calcium release under ER stress using Rhod 2-AM, a cell-permeable fluorescent Ca^{2+} indicator that detects kinetic changes in calcium concentration. This probe possesses a positive charge and is a mitochondrial-selective Ca^{2+} indicator [25, 26]. Therefore, Rhod 2-AM fluorescence intensity indicates the mitochondrial concentration of Ca^{2+} and reflects the release of Ca^{2+} from the ER and subsequent transfer to the mitochondria under ER stress. After treatment with H_2O_2, fluorescence microscopy results showed that the increment of fluorescence intensity of the ALR-OE group was significantly less than that of the vector group, indicating less mitochondrial calcium accumulation in the ALR-OE group (Fig. 7a, b) ($p < 0.05$). Consistent with the microscopy results, kinetic measurement using a Thermo multimode microplate reader showed a slow increase in Ca^{2+} concentrations in both groups (Fig. 7c). However, the overexpression of ALR led to a slower increase of Ca^{2+} concentration compared with that of the vector group (Fig. 7c, d). A bar graph showed the increment of the fluorescence intensity from 0 to 10 min in the vector group was significantly stronger than that of the ALR-OE group (Fig. 7d) ($p < 0.05$). These results indicate that the overexpression of ALR inhibits Ca^{2+} transfer from the ER to the mitochondria.

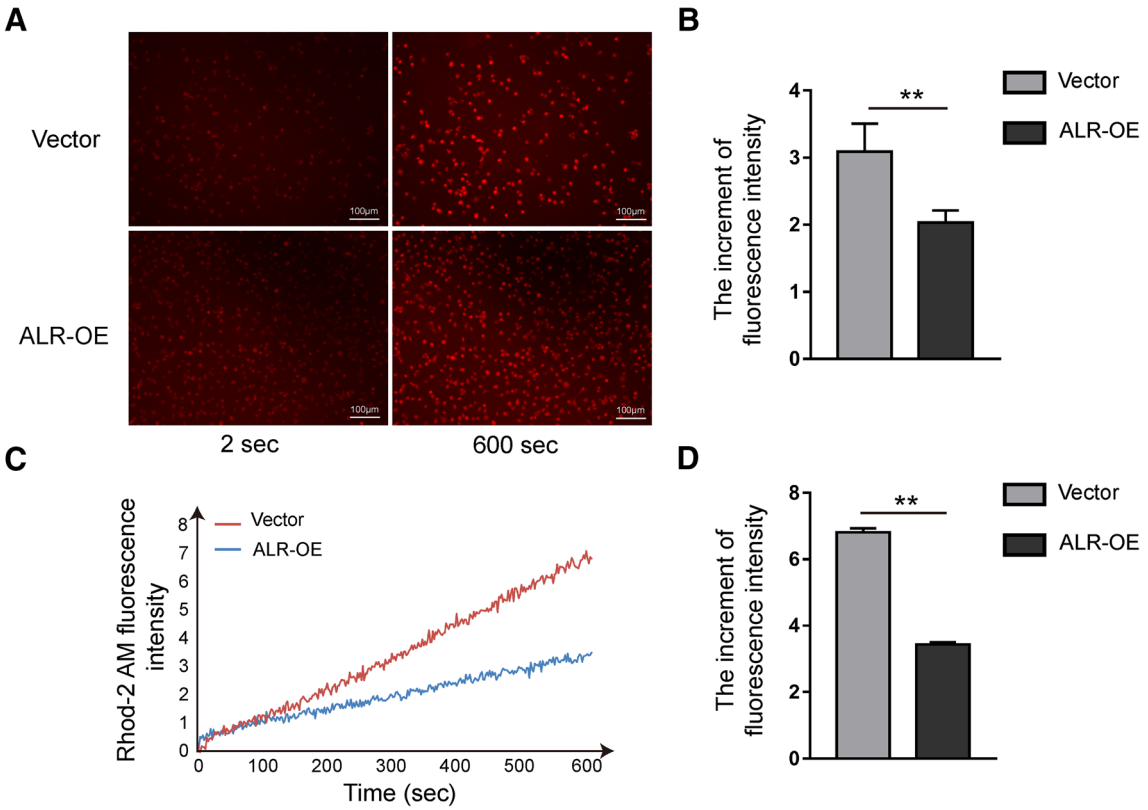

Fig. 7 Effect of ALR on calcium release under ER stress. **a** Rhod 2-AM was used to detect the calcium of mitochondria in the ALR-OE group and vector group treated with 200 μM H_2O_2 for 12 h. The images represent the first (2 s) and the last (600 s) picture taken by fluorescence microscope in a continuous detection (every 2 s for 10 min). **b** The bar graph show the increment of the fluorescence intensity from 2 to 600 s in ALR-OE group and vector group. **c** A kinetic measurement of calcium in ALR-OE group and vector group is visualized by kinetic curve of baseline-structured fluorescence values; average of three replicates. **d** The bar graph showed the increment of the fluorescence intensity from 0 to 600 s in ALR-OE group and vector group. ** means $p < 0.01$

Discussion

Ischemia/reperfusion induced apoptosis is associated with ER stress in various organs, including the kidney. While ALR is reported to have a protective role in H_2O_2-induced apoptosis in AKI, the mechanism underlying this effect remains unclear. In this study, we investigated the role of ALR in H_2O_2-induced ER stress-mediated apoptosis.

The ER is a multifunctional membranous organelle responsible for protein folding and calcium homeostasis [10]. In the present study, the confocal results showed that the staining pattern of ALR shares almost an identical distribution with that of ER in the vector group or in the ALR-OE group. Moreover, Western blots showed that ALR was detected in the ER fraction. These results indicated that ALR is expressed in the ER of HK-2 cells. We thus further explored the link between ALR and ER function. The ER is very vulnerable to stress like I/R, the major cause of acute kidney injury. When suffering from I/R, the overproduction of ROS leads to accumulation in the renal tubule epithelial cells, thus leading to oxidative stress-induced ER stress [27]. Our previous study showed that the expression of ALR was increased in a rat model of renal ischemia/reperfusion [17]. Consistently, in the present study, we found that the expression of ALR was increased at 12 h in the process of H_2O_2-induced ER stress. The decrease of ALR expression at 48 h compared with 12 h is maybe affected by the condition of the culture medium which causes most of the cells become unviable. This result indicated that ALR may take part in the process of H_2O_2-induced ER stress. The production of ROS has been reported to be a cause and also a consequence of ER stress, and ROS is the initiator of the mitochondrial pathway of apoptosis [28]. Therefore, ROS is an important modulator of ER stress-induced mitochondrial apoptosis. In the present study, we found that the overexpression of ALR reduced the levels of intracellular ROS in HK-2 cells under ER stress induced by H_2O_2. This indicated that ALR attenuates the oxidative environment by reducing ROS levels. As ER stress continues, the abnormal protein accumulates in the lumen of ER, thus destroying the normal morphology of the ER [29]. Through TEM, we found that ALR attenuated the dilation of the ER under H_2O_2 insult.

This observation indicated that ALR may play a protective role in ER stress.

GRP78 is the most abundant ER chaperone, and acts as the gatekeeper for mammalian UPR [30]. When ER stress occurs, UPR is activated by the dissociation of GRP78 from ER membrane sensors. Therefore, GRP78 is regarded as the marker and major regulator of ER stress [31]. Furthermore, the PERK pathway is the major pathway of ER stress-induced apoptosis in kidney injury [32]. In a previous study, Verfaillie et al. found that loss of PERK may cause defects in cell death sensitivity in pathological conditions linked to ROS-mediated ER stress [33]. Moreover, the transcription factor CHOP, downstream of PERK, is a critical mediator of ER stress-induced apoptosis [11]. Noh et al. previously found that CHOP deficiency attenuated renal ischemia/reperfusion injury in mice [8]. In the present study, we found that ALR reduced the expression of GPR78, the downstream phosphorylation of PERK and eIF2α and the activation of CHOP. Through flow cytometry, we found that ALR reduced the apoptotic cell rate in ER stress. These data suggest that ALR attenuates ER stress-apoptosis by suppressing the unfolded protein response through the PERK–eIF2α–CHOP pathway. Apoptosis is triggered through two signaling pathways, the extrinsic and intrinsic pathway. The intrinsic pathway is also known as the mitochondrial pathway [34]. A recent study suggests that CHOP regulates the intrinsic apoptosis pathway by inhibiting the Bcl-2 family [35], including anti-apoptotic protein Bcl-2 and the proapoptotic protein Bax. During metabolic disorders, the mitochondrial outer membrane is permeabilized, and Bax is activated, resulting in the release of cytochrome c and the subsequent activation of the caspase-dependent pathway, ultimately leading to apoptosis [36]. In the present study, we found that in H_2O_2 induced ER stress, the overexpression of ALR downregulated Bax expression and upregulated Bcl-2 expression compared to the vector group. Thus, the Bax/Bcl-2 ratio in the ALR-OE group was decreased compared to the vector group. Furthermore, the overexpression of ALR downregulated the levels of cleaved-caspase-3 compared with the vector group. These data demonstrated that ALR inhibits ER stress-induced apoptosis via the CHOP mediated pathway.

Calcium homeostasis disequilibrium is another important mediator that causes ER-stress apoptosis. As ER stress sustained, Ca^{2+} is released from the ER stores and loads into the mitochondria causing the mitochondrial Ca^{2+} level to overload; this triggers the loss of mitochondrial membrane potential and the subsequent release of cytochrome c. The release of cytochrome c, and the dominant position of Bax, ultimately lead to apoptosis [37]. The transfer of calcium from the ER to mitochondria is the initial trigger of ER stress-mediated apoptosis. Deniaud et al. previously reported that data acquired by Rhod 2-AM showed a higher sustained increase in mitochondrial Ca^{2+} concentration when treated with an inhibitor of SERCA (sarco/endoplasmic reticulum Ca^{2+}-ATPase) pumps [38]. Similarly, in the present study, we found that under ER stress, the Ca^{2+} concentration of mitochondria resulted in a lower sustained increase in the ALR overexpression group than that of the vector group. These data indicate that ALR may reduce the transfer of calcium from the ER to the mitochondria, and hence inhibit the calcium-dependent mitochondrial apoptosis pathway in ER stress.

To conclude, our research provides evidence that ALR attenuates ER stress-mediated apoptosis caused by H_2O_2 by suppressing the ER stress response and by maintaining calcium homeostasis in HK-2 cells, thereby, playing a role in protecting renal tubule epithelial cells from ischemia/reperfusion induced acute kidney injury.

Acknowledgements This study was supported by grants from the National Natural Science Foundation of China (Grant Nos. 81873604 and 30971334), Natural Science Foundation Project of CQ CSTC (Grant No. cstc2015jcyjA10069), Medical Scientific Research Projects of Chongqing Health and Family Planning Commission (Grant No. 20142031) and The Found for Fostering Talents in Scientific Research of Chongqing Medical University (Grant No. 201404).

Compliance with ethical standards

Conflict of interest The authors declare no conflict of interest.

References

1. Zuk A, Bonventre JV (2016) Acute kidney injury. Annu Rev Med 67(1):293–307. https://doi.org/10.1146/annurev-med-050214-013407
2. Bellomo R, Kellum JA, Ronco C (2012) Acute kidney injury. Lancet 380(9843):756–766. https://doi.org/10.1016/s0140-6736(11)61454-2
3. Arai S, Kitada K, Yamazaki T, Takai R, Zhang X, Tsugawa Y, Sugisawa R, Matsumoto A, Mori M, Yoshihara Y, Doi K, Maehara N, Kusunoki S, Takahata A, Noiri E, Suzuki Y, Yahagi N, Nishiyama A, Gunaratnam L, Takano T, Miyazaki T (2016) Apoptosis inhibitor of macrophage protein enhances intraluminal debris clearance and ameliorates acute kidney injury in mice. Nat Med 22:183. https://doi.org/10.1038/nm.4012
4. Basile DP, Anderson MD, Sutton TA (2012) Pathophysiology of acute kidney injury. Compr Physiol 2(2):1303–1353. https://doi.org/10.1002/cphy.c110041
5. Dennis MJ, Witting KP (2017) Protective role for antioxidants in acute kidney disease. Nutrients. https://doi.org/10.3390/nu9070718
6. Ali I, Shah SZ, Jin Y, Li ZS, Ullah O, Fang NZ (2017) Reactive oxygen species-mediated unfolded protein response pathways in preimplantation embryos. J Vet Sci 18(1):1–9. https://doi.org/10.4142/jvs.2017.18.1.1
7. Qin C, Xiao C, Su Y, Zheng H, Xu T, Lu J, Luo P, Zhang J (2017) Tisp40 deficiency attenuates renal ischemia reperfusion injury induced apoptosis of tubular epithelial cells. Exp Cell Res 359(1):138–144. https://doi.org/10.1016/j.yexcr.2017.07.038

8. Noh MR, Kim JI, Han SJ, Lee TJ, Park KM (2015) C/EBP homologous protein (CHOP) gene deficiency attenuates renal ischemia/reperfusion injury in mice. Biochim Biophys Acta 1852(9):1895–1901. https://doi.org/10.1016/j.bbadis.2015.06.004
9. Chen BL, Sheu ML, Tsai KS, Lan KC, Guan SS, Wu CT, Chen LP, Hung KY, Huang JW, Chiang CK, Liu SH (2015) CCAAT-enhancer-binding protein homologous protein deficiency attenuates oxidative stress and renal ischemia-reperfusion injury. Antioxid Redox Signal 23(15):1233–1245. https://doi.org/10.1089/ars.2013.5768
10. Bravo-Sagua R, Rodriguez AE, Kuzmicic J, Gutierrez T, Lopez-Crisosto C, Quiroga C, Diaz-Elizondo J, Chiong M, Gillette TG, Rothermel BA, Lavandero S (2013) Cell death and survival through the endoplasmic reticulum-mitochondrial axis. Curr Mol Med 13(2):317–329. https://doi.org/10.2174/1566524011313020008
11. Oyadomari S, Mori M (2003) Roles of CHOP/GADD153 in endoplasmic reticulum stress. Cell Death Differ 11:381. https://doi.org/10.1038/sj.cdd.4401373
12. Zhou X, Hao W, Shi H, Hou Y, Xu Q (2015) Calcium homeostasis disruption—a bridge connecting cadmium-induced apoptosis, autophagy and tumorigenesis. Oncol Res Treat 38(6):311–315
13. Pinton P, Giorgi C, Siviero R, Zecchini E, Rizzuto R (2008) Calcium and apoptosis: ER-mitochondria Ca^{2+} transfer in the control of apoptosis. Oncogene 27:6407. https://doi.org/10.1038/onc.2008.308
14. Rizzuto R, Marchi S, Bonora M, Aguiari P, Bononi A, De Stefani D, Giorgi C, Leo S, Rimessi A, Siviero R, Zecchini E, Pinton P (2009) Ca^{2+} transfer from the ER to mitochondria: when, how and why. Biochim Biophys Acta (BBA) Bioenergetics 1787(11):1342–1351. https://doi.org/10.1016/j.bbabio.2009.03.015
15. Nalesnik MA, Gandhi CR, Starzl TE (2017) Augmenter of liver regeneration: a fundamental life protein. Hepatology 66(1):266–270. https://doi.org/10.1002/hep.29047
16. Hagiya M, Fracavailla A, Polimeno L, Ihara I, Sakai H, Seki T, Shimonishi M, Porter KA, Starzl TE (1994) Cloning and sequence analysis of the rat augmenter of liver regeneration (ALR) gene: expression of biologically active recombinant ALR and demonstration of tissue distribution. Proc Natl Acad Sci USA 91(17):8142–8146
17. Liao X-h, Zhang L, Liu Q, Sun H, Peng C-m, Guo H et al (2010) Augmenter of liver regeneration protects kidneys from ischaemia/reperfusion injury in ratsX. Nephrol Dial Transplant 25(9):2921–2929. https://doi.org/10.1093/ndt/gfq151
18. Tury A, Mairet-Coello G, Lisowsky T, Griffond B, Fellmann D (2005) Expression of the sulfhydryl oxidase ALR (augmenter of liver regeneration) in adult rat brain. Brain Res. https://doi.org/10.1016/j.brainres.2005.04.050
19. Gandhi CR (2012) Augmenter of liver regeneration. Fibrogenes Tissue Repair 5(1):10. https://doi.org/10.1186/1755-1536-5-10
20. Lange H, Lisowsky T, Gerber J, Mühlenhoff U, Kispal G, Lill R (2001) An essential function of the mitochondrial sulfhydryl oxidase Erv1p/ALR in the maturation of cytosolic Fe/S proteins. EMBO Rep. https://doi.org/10.1093/embo-reports/kve161
21. Sevier CS, Cuozzo JW, Vala A, Åslund F, Kaiser CA (2001) A flavoprotein oxidase defines a new endoplasmic reticulum pathway for biosynthetic disulphide bond formation. Nat Cell Biol 3:874. https://doi.org/10.1038/ncb1001-874
22. Polimeno L, Pesetti B, De Santis F, Resta L, Rossi R, De Palma A, Girardi B, Amoruso A, Francavilla A (2012) Decreased expression of the augmenter of liver regeneration results in increased apoptosis and oxidative damage in human-derived glioma cells. Cell Death Dis 3:e289. https://doi.org/10.1038/cddis.2012.25
23. Xia N, Yan RY, Liu Q, Liao XH, Sun H, Guo H, Zhang L (2015) Augmenter of liver regeneration plays a protective role against hydrogen peroxide-induced oxidative stress in renal proximal tubule cells. Apoptosis Int J Progr Cell Death 20(4):423–432. https://doi.org/10.1007/s10495-015-1096-2
24. Liu XR, Cao L, Li T, Chen LL, Yu YY, Huang WJ, Liu L, Tan XQ (2017) Propofol attenuates H_2O_2-induced oxidative stress and apoptosis via the mitochondria- and ER-medicated pathways in neonatal rat cardiomyocytes. Apoptosis Int J Progr Cell Death 22(5):639–646. https://doi.org/10.1007/s10495-017-1349-3
25. Hajnóczky G, Robb-Gaspers LD, Seitz MB, Thomas AP (1995) Decoding of cytosolic calcium oscillations in the mitochondria. Cell 82(3):415–424. https://doi.org/10.1016/0092-8674(95)90430-1
26. Babcock DF, Herrington J, Goodwin PC, Park YB, Hille B (1997) Mitochondrial participation in the intracellular Ca^{2+} network. J Cell Biol 136(4):833
27. Bonventre JV, Yang L (2011) Cellular pathophysiology of ischemic acute kidney injury. J Clin Investig 121(11):4210–4221. https://doi.org/10.1172/JCI45161
28. Boussabbeh M, Ben Salem I, Prola A, Guilbert A, Bacha H, Abid-Essefi S, Lemaire C (2015) Patulin induces apoptosis through ROS-mediated endoplasmic reticulum stress pathway. Toxicol Sci 144(2):328–337. https://doi.org/10.1093/toxsci/kfu319
29. Pluquet O, Pourtier A, Abbadie C (2015) The unfolded protein response and cellular senescence. A review in the theme: cellular mechanisms of endoplasmic reticulum stress signaling in health and disease. Am J Physiol Cell Physiol 308(6):C415–C425. https://doi.org/10.1152/ajpcell.00334.2014
30. Zhu G, Lee AS (2015) Role of the unfolded protein response, GRP78 and GRP94 in organ homeostasis. J Cell Physiol 230(7):1413–1420. https://doi.org/10.1002/jcp.24923
31. Fu XL, Gao DS (2014) Endoplasmic reticulum proteins quality control and the unfolded protein response: the regulative mechanism of organisms against stress injuries. BioFactors 40(6):569–585. https://doi.org/10.1002/biof.1194
32. Taniguchi M, Yoshida H (2015) Endoplasmic reticulum stress in kidney function and disease. Curr Opin Nephrol Hypertens 24(4):345–350. https://doi.org/10.1097/MNH.0000000000000141
33. Verfaillie T, Rubio N, Garg AD, Bultynck G, Rizzuto R, Decuypere JP, Piette J, Linehan C, Gupta S, Samali A, Agostinis P (2012) PERK is required at the ER-mitochondrial contact sites to convey apoptosis after ROS-based ER stress. Cell Death Differ 19(11):1880–1891. https://doi.org/10.1038/cdd.2012.74
34. Wu C-C, Bratton SB (2012) Regulation of the intrinsic apoptosis pathway by reactive oxygen species. Antioxid Redox Signal 19(6):546–558. https://doi.org/10.1089/ars.2012.4905
35. Iurlaro R, Muñoz-Pinedo C (2015) Cell death induced by endoplasmic reticulum stress. FEBS J 283(14):2640–2652. https://doi.org/10.1111/febs.13598
36. Sano R, Reed JC (2013) ER stress-induced cell death mechanisms. Biochim Biophys Acta 1833(12):3460–3470. https://doi.org/10.1016/j.bbamcr.2013.06.028
37. Qiao Y, Wang C, Xu K, Meng L, Li X, Pei X, Wang J, Meng H, Zeng L (2014) Changes in calcium/calmodulin level and mitochondrial membrane potential in cochlear neurons of newborn mice infected with murine cytomegalovirus. Cell Biochem Biophys 69(3):593–598. https://doi.org/10.1007/s12013-014-9838-2
38. Deniaud A, Sharaf el dein O, Maillier E, Poncet D, Kroemer G, Lemaire C, Brenner C (2008) Endoplasmic reticulum stress induces calcium-dependent permeability transition, mitochondrial outer membrane permeabilization and apoptosis. Oncogene 27(3):285–299. https://doi.org/10.1038/sj.onc.1210638